JOURNAL OF CATALYSIS 150, 376–387 (1994)

Selective Reduction of NO_x by Methane on Co–Ferrierites

I. Reaction and Kinetic Studies

Yuejin Li and John N. Armor

Air Products and Chemicals, Inc., 7201 Hamilton Boulevard, Allentown, Pennsylvania 18195

Received April 4, 1994; revised August 16, 1994

Cobalt-exchanged ferrierite zeolite catalysts were found to be very active (about twice the activity compared to Co–ZSM-5) for the selective reduction of NO_x with CH_4. The presence of oxygen (gaseous O_2 or O atoms via N_2O decomposition) greatly enhanced the NO_x conversion to N_2. In the absence of O_2, NO_2 can be effectively reduced with CH_4, but its conversion decreased with increasing temperature at $T > 500$°C with a formation of small amount of O_2. Temperature programmed desorption measurements show that the presence of O_2 alters the NO adsorption/desorption on Co–ferrierite, yielding an additional, high-temperature NO desorption peak. Partial pressure dependencies were measured as a function of reaction temperature under both dry and wet conditions. In the absence of added H_2O vapor, the empirical reaction order with respect to NO (0.2 to 0.4) increased with increasing temperature with no change in the reaction order for CH_4 (0.7). Addition of H_2O vapor (2%) significantly increased the empirical reaction orders with respect to both NO (0.7) and CH_4 (0.8–0.9). Under wet conditions, the reaction orders are higher at low temperatures. The added H_2O vapor also substantially raised the apparent activation energies for both NO reduction and CH_4 combustion. The turnover frequencies for both reactions increased with increasing Co^{2+} level, demonstrating the heterogeneity of the Co^{2+} sites. The differences in activity and selectivity and in the distribution of active sites between Co–ferrierite and Co–ZSM-5 may be related to the different channel systems of these two zeolites.

INTRODUCTION

The use of hydrocarbons to catalytically reduce NO_x emission is an attractive approach for some emission sources. Compared to the commercially practiced selective catalytic reduction (SCR) process which uses ammonia, this approach provides some advantages, i.e., elimination of the problems associated with the use of ammonia (transportation and storage, equipment corrosion, and ammonia slip). When methane is used as a reductant for NO_x, it offers better system integration because natural gas (mainly methane) is readily available and is widely used as a fuel for many electrical utilities and stationary combustion engines.

Effective reduction of NO_x using methane in the presence of excess oxygen was first reported by Li and Armor over a Co^{2+}-exchanged ZSM-5 catalyst (1) and subsequently on other metal- (Mn^{2+} and Ni^{2+}) exchanged zeolites (ZSM-5 and mordenite) (2). Contrary to the unselective nature of methane (its preference to combustion) reported previously with other catalysts (3, 4), on a Co–ZSM-5 catalyst , NO was selectively reduced to N_2 in the presence of excess O_2. In fact, the presence of O_2 greatly enhanced the NO reduction. The NO conversion is proportional to the level of CH_4 in feed, and 100% NO conversion to N_2 at 400°C was reported with a Co–ZSM-5 catalyst (1). Based on product analysis and the fact that O_2 is essential for the NO reduction, the stoichiometry for NO reduction is described by Eq. [1]. Two parallel catalytic reactions occur on the catalyst, i.e., NO reduction (Eq. [1]) and CH_4 combustion (Eq. [2]). The novelty of these metal exchanged catalysts is their ability to catalyze the NO reduction in excess O_2 while minimizing the CH_4 combustion (Eq. [2]):

$$2NO + CH_4 + O_2 \rightarrow N_2 + CO_2 + 2H_2O \quad [1]$$

$$CH_4 + 2O_2 \rightarrow CO_2 + 2H_2O. \quad [2]$$

The NO reduction activity was found to be proportional to the Co^{2+} exchange level in Co–ZSM-5, and the parent zeolite, Na–ZSM-5, is inactive (1). Therefore, the transition metal ions, e.g., Co^{2+}, exchanged into the zeolite must be responsible for the NO reduction. Interestingly, NO cannot be effectively reduced by CH_4 on Cu–ZSM-5 in the presence of O_2, where CH_4 combustion (Eq. [2]) dominates (2). It is well known that Cu–ZSM-5 is a unique catalyst for the direct decomposition of NO to its elements (5, 6) and is active for the selective reduction of NO with higher hydrocarbons, e.g., C_2H_4 (7, 8), C_3H_6 (9–12), C_3H_8 (4, 13, 14), and i-C_4H_8 (15). In fact, in the *absence* of

0021-9517/94 $6.00

O_2, Cu–ZSM-5 is very active for the NO reduction with CH_4 (1).

More recently, metal-exchanged ferrierite was reported to be a more active catalyst for reaction [1] (16); the activity for the NO reduction on Co–ferrierite was twice that for Co–ZSM-5 at 500°C. The role of zeolite in influencing the Co^{2+} activity is exemplified by comparing Co–Y (the least active), Co–ZSM-5, and Co–ferrierite (the most active). Shape selectivity of zeolite does not appear to be important for this reaction because the reactants are relatively small molecules, and acidity is not essential for CH_4 as a reductant. Factors like cation coordination and relative diffusivity in different zeolites appear to be more important. In the past, we explored many catalytic systems for the $NO/CH_4/O_2$ reaction, but the mechanism and state of catalyst were not described in detail. The objective of this work is to better understand this catalytic system. In this paper, we present data on reaction and kinetic studies over Co^{2+}-exchanged ferrierites and address the role of oxygen on reaction rate and the intrinsic activity of each Co^{2+} ion in the zeolite. The difference in catalytic properties among various Co–zeolite catalysts, especially between Co–ZSM-5 and Co–ferrierite, can be rationalized based on zeolite topology. In a companion paper, we use catalyst characterization and activity data to discuss a reaction mechanism for the NO reduction with CH_4 (17).

EXPERIMENTAL

A Co–ferrierite catalyst was prepared via a two-step exchange process. A mixed cation (K^+, Na^+) ferrierite (obtained from TOSOH Corporation, Japan) was first converted to NH_4^+ form by exchanging with NH_4NO_3; the NH_4^+ form was then exchanged with Co^{2+} to obtain Co–ferrierite. The details of the exchange are described elsewhere (16). The ferrierite zeolites used have two Si/Al ratios (~6 and ~8), and they are expressed as FER(6) and FER(8), respectively. The Co^{2+} exchange level is expressed as a percentage of the exchange capacity (exchange level = Co/Al × 2 × 100); Co/Al = 0.5 means that Co^{2+} is 100% exchanged. Consequently, Co–FER(8)-78 means that the Co–ferrierite sample has Si/Al = 8 and Co/Al = 0.39 (or 78% exchanged). Elemental analyses were performed by using atomic absorption spectroscopy (for Na) and inductively coupled plasma-atomic emission spectroscopy (for Si, Al, and Co). To standardize on a weight basis, a sample was equilibrated at 53% of relative humidity at room temperature before the elemental analyses.

The typical experimental procedures for activity measurements were described previously (1, 2). Briefly, the activities were measured using a microcatalytic reactor operating in a steady-state plug-flow mode. The reactor was a U-shaped quartz tube with $\frac{1}{4}$ in. o.d. in the inlet section and $\frac{3}{8}$ in. o.d. in the outlet section. The catalyst bed was located in the outlet section and packed between quartz wool plugs. A catalyst was pelletized, crushed, and then sieved to 60–80 mesh before loading into the reactor. A catalyst was routinely pretreated *in situ* in flowing He at 500°C for 1 h at a ramp rate of 5°C/min. The reaction mixture was obtained by blending four channels of flow, i.e., NO/He, CH_4/He, O_2/He, and He, and each was controlled by an independent mass flow controller. Thus, various feed compositions were obtained and will be described in conjunction with the results. A total flow rate of 100 cm^3/min. and a 0.1-g sample were used to study the effect of feed composition (Tables 1 and 2). A zeolite sample was weighed without any precaution to avoiding moisture. [Samples had been stored at room temperature in sample vials.] Therefore, GHSV for these studies was 30,000 based on an apparent bulk density of

TABLE 1

Effect of O_2 on NO_x Conversion over Co–FER(6)[a]

Conditions[b]	400°C	450°C	500°C	550°C
1600 ppm NO, O_2 free	6	7	8	10
1600 ppm NO, with 2.5% O_2	11	33	50	40
960 ppm NO_2, O_2 free	22	37	42	33
960 ppm NO_2, with 2.5% O_2	n.a.	n.a.	56	n.a.

[a] This catalyst has the following composition: Si/Al = 6, Co/Al = 0.37.

[b] For all experiments, [CH_4] = 1000 ppm, GHSV = 30,000.

TABLE 2

Empirical Reaction Orders in NO and CH_4 under Dry and Wet Conditions on Co–FER(6)[a]

Variable	Condition	400°C	425°C	450°C	475°C	500°C
NO[b]	Dry	0.24	0.19	0.23	—	0.38
	Wet	—	—	0.74	—	0.71
CH_4[c]	Dry	0.74	0.73	0.72	—	0.73
	Wet	—	—	0.92	0.76	0.75

[a] This catalyst has the following composition: Si/Al = 6, Co/Al = 0.37.

[b] Dry conditions: NO partial pressure dependence was measured with 975 ppm CH_4 and 2.5% O_2 at GHSV of 50,000 (400–450°C) and 100,000 (500°C). Wet conditions: 975 ppm CH_4, 2.5% O_2, 2% H_2O, and GHSV = 30,000. [NO] varied from 600 to 1600 ppm.

[c] Dry conditions: CH_4 partial pressure dependence was measured with 805 ppm NO and 2.5% O_2 at GHSV of 100,000 (400–450°C) and 200,000 (500°C). Wet conditions: 805 ppm NO, 2.5% O_2, 2% H_2O, and GHSV = 30,000. [CH_4] varied from 400 to 2000 ppm.

the zeolite catalyst, ~0.5 g/cm^3. For some kinetic runs higher space velocities (GHSV = 100,000–200,000) were used to obtain low conversions. [Here, the conversions were maintained below 30%.]

For reaction runs involving addition of water vapor, the He feed was saturated with H_2O via a saturator composed of a sealed glass bubbler with a medium-pore frit immersed into deionized H_2O. The bubbler was surrounded by a heating tape and insulated by glass wool. The temperature of the bubbler was controlled by a temperature controller. Different amounts of H_2O could be added to the feed by adjusting the bubbler temperature. To avoid any condensation of H_2O vapor, the stainless steel line containing H_2O vapor was heat traced at a temperature higher than the saturation temperature. To protect GC column from excessive H_2O, an ice-cooled H_2O condenser was incorporated right after the reactor to condense out most of the H_2O vapor.

An on-line gas chromatograph with a TCD detector was used for the product analysis, and a molecular sieve 5 Å column was used to separate N_2, O_2, and CH_4. Earlier we demonstrated (1, 2) that no other by-products were produced beyond those given by Eqs. [1] and [2]. For both NO and NO_2 reduction, formation of N_2 was used to calculate NO or NO_2 conversion, and the CH_4 conversion was obtained by following the change in CH_4 peak area. A steady-state NO reduction rate (mol/g h) is calculated as

$$\text{NO reduction rate} = -\frac{d[\text{NO}]}{dt} = \frac{F_{\text{NO}} \times \text{Con}_{\text{NO}}}{W \times 100}, \quad [3]$$

where F_{NO} is the flow rate of NO (mol/h), Con_{NO} is the conversion of NO in percent, and W is the weight of a catalyst. The CH_4 consumption rate can be calculated in a similar fashion, except F_{CH_4} and Con_{CH_4} are used. Turnover frequency (TOF) is obtained by the ratio of the rate (from Eq. [3]) to the Co^{2+} level and has a unit of 1/sec.

Three separate temperature programmed desorption (TPD) measurements were made in various streams (He, O_2/He mixture, and O_2/CH_4/He mixture) to study the effect of O_2 and O_2/CH_4 mixture on the NO adsorption/desorption. TPD of NO was carried out in the same reactor system (without the H_2O trap) with a 0.1-g sample (~0.5 cm deep and 0.7 cm in diameter). A Co–FER(6) sample was pretreated *in situ* at 500°C in flowing He for 1 h, then was cooled to 25°C in He. The NO adsorption was carried out at 25°C by flowing a NO/Ar/He mixture (1700 ppm NO, 2500 ppm Ar, 100 cm^3/min.) through the sample bed. The effluent of the reactor was continuously monitored by a mass spectrometer (UTI 100C), and the leveling off in NO intensity indicated the saturation of the sample with NO. [The small quantity of Ar in the mixture was used as an inert tracer.] A period of ~30 min is sufficient to achieve a saturation for NO adsorption. During NO adsorption, no appreciable amount of other species was observed. After the NO adsorption, the sample was then flushed with a stream of He (100 cm^3/min) at 25°C to eliminate gaseous NO and weakly adsorbed NO. As the gaseous NO level, monitored by the mass spectrometer, returned to near the background level of the mass spectrometer, the sample was heated to 500°C at a ramp rate of 8°C/min in flowing He (100 cm^3/min). [For TPD studies in alternative streams, O_2/He or O_2/CH_4/He was turned on after flushing with He at room temperature.] The desorbed species were monitored continuously by the mass spectrometer as a function of time/temperature. The mass spectrometer was calibrated for N_2, O_2, NO, N_2O, and other relevant species, and therefore quantitative analysis was possible. The amount of the NO adsorbed on catalyst can be obtained from either a NO adsorption measurement (by integrating NO uptake) or from a TPD profile (by integrating the desorption rate vs time).

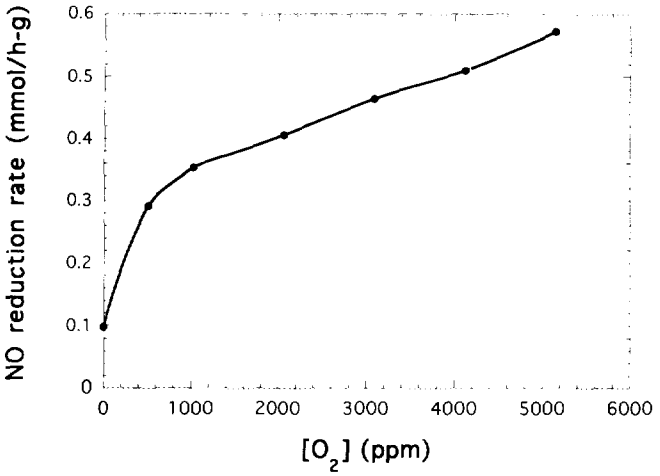

FIG. 1. Effect of O_2 on NO reduction rate over Co–FER(6)-74 at 450°C.

RESULTS

Figure 1 shows the dependence of NO reduction rate on the inlet O_2 concentration over a Co–FER(6) catalyst at 450°C. Upon addition of 600 ppm O_2 while keeping [NO] and [CH_4] constant, the NO reduction rate increased from 0.1 to 0.3 mmol/g h. Upon further increasing O_2 concentration, the rate continued to increase linearly up to 5200 ppm O_2. The enhancing effect of O_2 on this NO/CH_4 reaction was previously reported on Co–ZSM-5 and other catalysts (1, 2), and the presence of O_2 also promotes NO reduction with other reducing agents such as C_2H_4, C_3H_6, and C_3H_8 (7, 8, 18–22). To test the hypothesis that

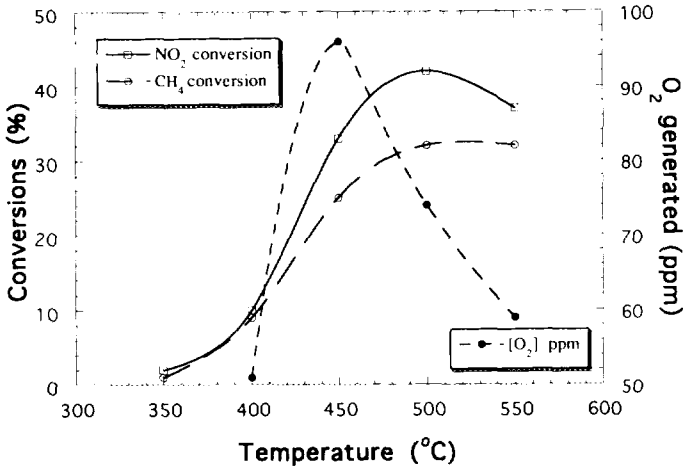

FIG. 2. NO_2 reduction by CH_4 in the absence of O_2 on Co–FER(8)-78. This reaction was run with a feed containing 0.55% NO_2 and 0.56% CH_4 and at a GHSV = 30,000. The NO_2 conversion was calculated based on N_2 formation.

NO_2 species may be formed by reacting NO with O_2 and that the NO_2 species may be an intermediate for the NO reduction, an experiment using NO_2 as a reactant was carried out. As shown in Table 1, in the absence of O_2, NO_2 can be effectively reduced with CH_4 on Co–FER(6); 42% NO_2 conversion was obtained at 500°C, which is in a clear contrast to NO under the same conditions. Addition of 2.5% O_2 to this NO_2 containing feed at 500°C increased NO_2 conversion to 56%.

The NO_x conversion can also be enhanced by the presence of N_2O. Addition of 1000 ppm N_2O in a feed containing only NO (850 ppm) and CH_4 (1000 ppm) in the absence of O_2 greatly enhanced the NO conversion (from 8 to 47%) on a Co–FER(8) catalyst at 500°C. Here N_2O might serve as an oxygen source. The oxygen may participate the reaction as gas-phase O_2 molecules resulting from the decomposition of N_2O (22). However, even if the N_2O was completely converted to N_2 and O_2, there was only 500 ppm O_2 available, and such a low level of O_2 should not yield the degree of enhancement observed (see Fig.1). More likely, N_2O supplies catalyst bound oxygen atoms via its dissociation, and these oxygen atoms are highly reactive with NO forming NO_2 on catalyst. Thus, N_2O is a very efficient source of oxygen for the selective reduction of NO. A similar observation was made over a Co–ZSM-5 catalyst (23). Further addition of 2.5% O_2 to this $NO/N_2O/CH_4$ mixture increased the NO conversion to 60%.

Figure 2 illustrates the results of NO_2 reduction with CH_4 in the absence of O_2 as a function of reaction temperature. The NO_2 conversion–temperature profile, resembling that for NO reduction in the presence of O_2 (1), displays a volcano-shaped curve with the maximum NO conversion (to N_2) of 42% at 500°C. The CH_4 conversion, on the other hand, levels off (32%) at $T > 500$°C. During this reaction O_2 was generated, and a plot of concentration also displays a volcano-shaped curve with its maximum at 450°C (97 ppm). Note that the amount of CH_4 consumed (32% at 500°C) is more than that required to reduce NO_2 to N_2 based on Eq. [4] (21% at 500°C).

$$2NO_2 + CH_4 \rightarrow N_2 + CO_2 + 2H_2O \quad [4]$$

$$NO_2 = NO + \tfrac{1}{2}O_2. \quad [5]$$

This suggests that some NO_2 was decomposed to NO and O_2 at higher temperatures (Eq. [5]), and this reaction is equilibrium limited and is strongly dependent on temperature (24). Some of the O_2 formed reacted with CH_4 forming combustion products via Eq. [2], which causes 11% of excess conversion of CH_4 at 500°C. [Since only 42% of NO_2 was reduced to N_2 at 500°C, abundant oxygen should be available (via Eq. [5]) for the CH_4 combustion.]

NO adsorption at room temperature and its TPD profiles were measured on Co–FER(6)-74. The amount of NO adsorbed at room temperature in 1700 ppm NO/He mixture was measured as 1.2 ± 0.1 mmol/g or 1.5 ± 0.1 NO/Co. Figure 3a shows the TPD profile measured in He. Three distinct NO desorption peaks were observed at ~75, 150, and 295°C, and a shoulder was seen at ~260°C. Concomitantly, three N_2 peaks were observed at the same temperatures, and the N_2 peak with the highest intensity was detected at ~75°C. This indicates that some NO molecules were stoichiometrically decomposed to N_2 and O_2 during the TPD measurement. However, the product O_2 was not desorbed from the catalyst. In addition, a broad N_2O peak was observed at ~295°C with a shoulder at ~250°C, suggesting that some NO also disproportionated to N_2O and NO_2 at elevated temperatures. NO_2 formed on catalyst may decompose to NO and O upon desorption with the oxygen atoms attaching to catalyst. Moreover, if gas-phase NO_2 was produced, it would be severely fragmented to NO in the mass spectrometer chamber during its ionization. All NO_x species were desorbed below 300°C. The amount of NO adsorbed is equivalent to 1.0 NO/Co, that of N_2 formation is equivalent to 0.2 NO/Co (1 molec. N_2 = 2 molec. NO), and that of N_2O is equivalent to 0.3 NO/Co. The total number of N atoms obtained from the TPD measurement is 1.5 N/Co, which is identical to that obtained by the adsorption measurement.

Figure 3b shows the TPD profile measured in flowing O_2/He mixture. For NO desorption, the high temperature peak at ~295°C completely disappeared, but a low-intensity peak, which may be a shoulder in Fig. 3a, was observed at ~220°C. The NO desorption corresponds to 1.3 NO/Co. The N_2 peaks are similar to those in Fig. 3a in both shape and quantity (equivalent to 0.3 NO/Co).

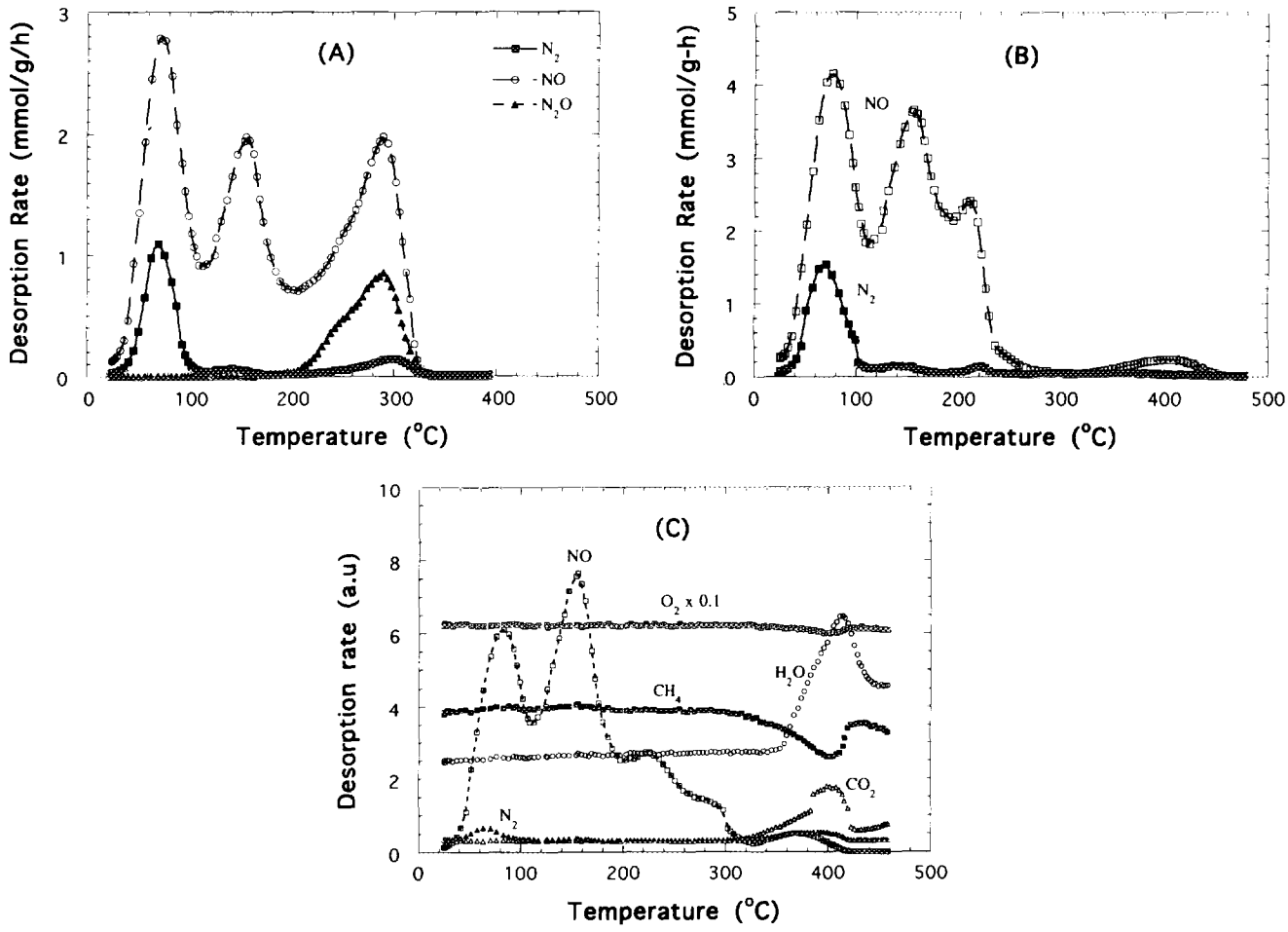

FIG. 3. Temperature programmed desorption and reaction over a Co–FER(6)-74 catalyst. (A) TPD of NO in flowing helium; (B) TPD of NO in a flowing O_2/He mixture (10% O_2); (C) TPD (TPRx) of NO in a flowing CH_4 (1000 ppm)/O_2 (2.5%)/He mixture.

However, N_2O desorption was not observed. This suggests that the presence of O_2 suppresses the disproportion reaction. Interestingly, a broad peak was found at ~400°C. Apparently, the adsorption strength of NO_x was enhanced by O_2.

Figure 3c shows the TPD profile measured in flowing O_2/CH_4/He mixture. In essence this is a temperature programmed reaction. At $T < 300$°C, the NO desorption features are similar to that shown in Fig. 3b. However, the quantity of N_2 formation is much smaller. At $T > 300$°C, besides a broad NO desorption peak (~370°C), N_2, CO_2, and H_2O formation was observed. Visible consumption of CH_4 and O_2 and formation of CO_2 and N_2 began at 300°C and peaked at 400°C. [Note that the O_2 signals were reduced 10 times in order to compare with other signals in the same plot.] The H_2O peak began to appear at 360°C and peaked at 420°C. The delay for H_2O peak appearance compared to other components is due to the relatively strong adsorption of H_2O on zeolite. At ~420°C, the N_2 formation became insignificant due to the depletion of surface NO_x species. [The N_2 signal returned to the background level.] Similarly, CO_2 and H_2O formation and CH_4 consumption dropped significantly at 420°C. But at $T > 420$°C, the CO_2 and H_2O formation as well as CH_4 consumption gradually increased with increasing temperature. Consistent with the steady-state data, at lower temperatures the main reaction was NO reduction not CH_4 combustion. At $T > 420$°C the extent of CH_4 combustion gradually increased. This experiment suggests that NO_x adsorption is necessary for the NO reduction, and at low temperatures activation of CH_4 or surface reaction is a rate-determining step for the NO reduction.

The kinetic studies presented in this section were made on Co–FER(6) (Si/Al = 6, Co/Al = 0.38). Figures 4 and 5 show partial pressure dependencies of NO reduction rate [in CH_4 and in NO] under dry feed conditions. The dependencies are also depicted as a function of reaction temperature. As companion results, the empirical reac-

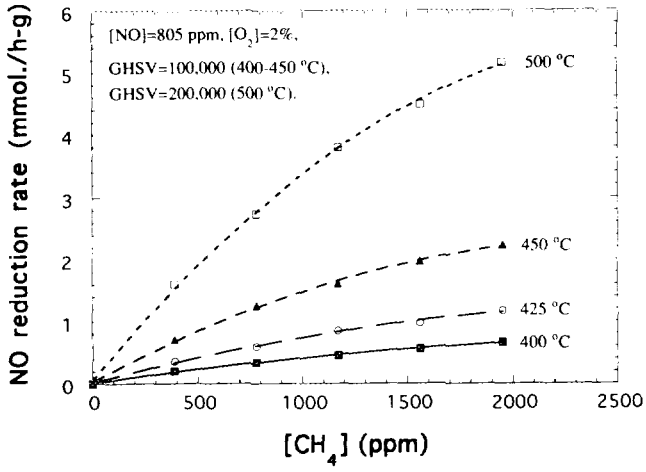

FIG. 4. The dependence of NO reduction rate on CH_4 concentration over Co–FER(6)-74 with a dry feed.

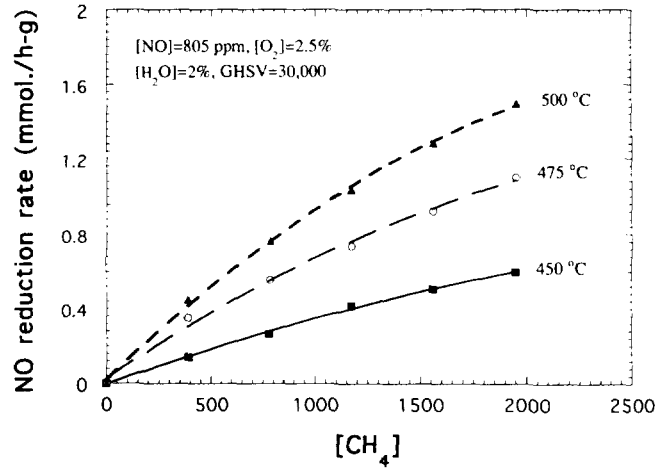

FIG. 6. The dependence of NO reduction rate on CH_4 concentration over Co–FER(6)-74 with a wet feed.

tion orders with respect to both NO and CH_4 are listed in Table 2. Under dry conditions, the NO reduction rate is proportional to the CH_4 level, and the dependence is stronger at higher temperatures (Fig. 4). Yet the empirical reaction order with respect to CH_4 is constant (~0.73 between 400 and 500°C) (Table 2). Generally, the NO reduction rate increases slightly with increasing NO concentration at T = 400–500°C (Fig. 5). Consequently, the reaction order with respect to NO is very low with the highest value 0.38 at 500°C. Similar to Co–ZSM-5, addition of 2% water vapor in the feed reduced the NO reduction rate but enhanced the concentration dependence (Figs. 6 and 7). As a result, the reaction orders increased significantly. The order with respect to NO increased from 0.23 to 0.74 at 450°C and from 0.38 to 0.71 at 500°C, whereas the order for CH_4 increased from 0.72 to 0.92 at 450°C and from 0.73 to 0.75 at 500°C (Table 2). Recall that with Co–ZSM-5, the reaction orders for both NO and CH_4 in a wet stream were ~1 (25).

The effect of H_2O on the apparent activation energy for NO reduction is shown in Fig. 8. The apparent activation energy in the absence of added H_2O is 22 kcal/mol which was obtained with 805 ppm NO, 1950 ppm CH_4, 2.5% O_2 and with a GHSV of 100,000. [Note that the Arrhenius plot under dry conditions does not bend over with increasing temperature. This is due to the low conversions of CH_4 with the high space velocity used.] In the presence of 2% H_2O, in addition to the much lower reaction rate, the activation energy increased to 34 kcal/mol. With extrapolation, the two lines would merge at ~600°C, where the

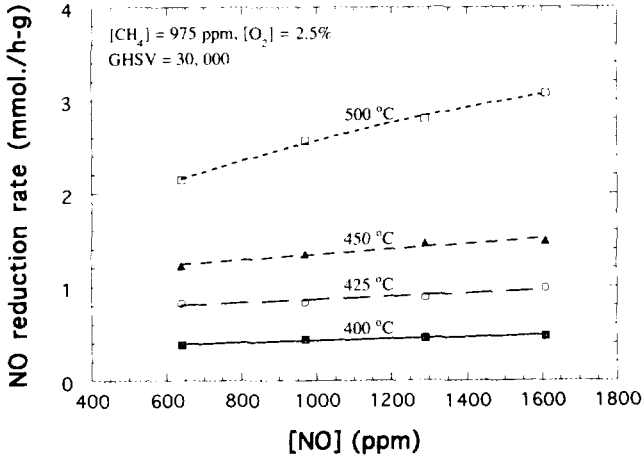

FIG. 5. The dependence of NO reduction rate on NO concentration over Co–FER(6)-74 with a dry feed.

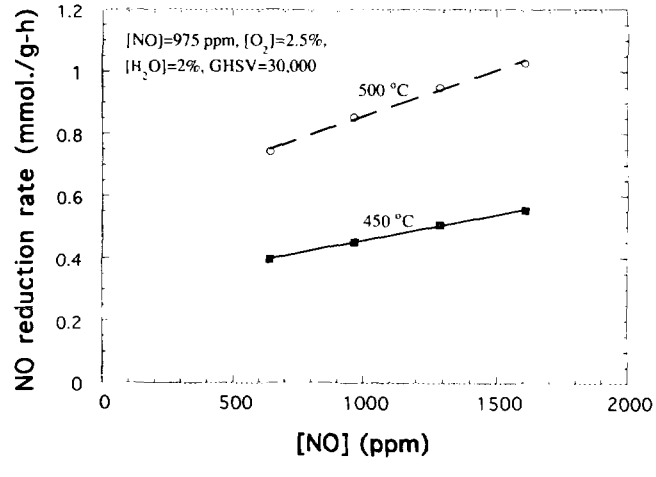

FIG. 7. The dependence of NO reduction rate on NO concentration over Co–FER(6)-74 with a wet feed.

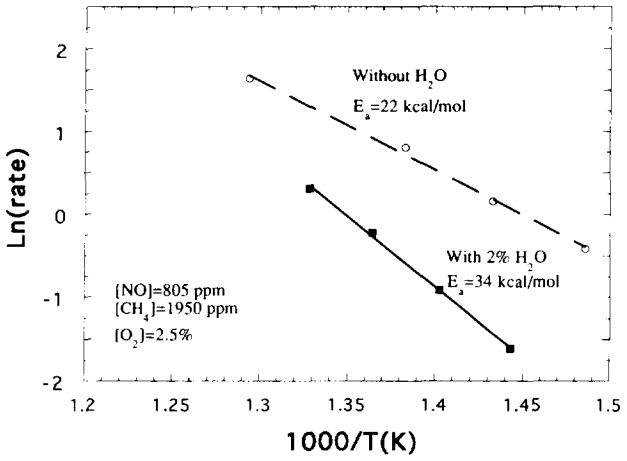

FIG. 8. Effect of H_2O on the activation energy for NO reduction over Co–FER(6)-74.

effect of water would be insignificant, which was observed (16).

The presence of H_2O not only changes the NO reduction rate and kinetics but also alters the CH_4 combustion rate. Relatively speaking, Co–ferrierite catalyst is not very active for the CH_4 combustion ($CH_4 + O_2$) at $T < 550$°C. In the presence of 2% water vapor, the CH_4 conversion is even lower; the conversion is only 5% at 500°C (GHSV = 30,000) (Fig. 8). Water has a similar impact on its kinetics; the apparent activation energy increased substantially (11 to 39 kcal/mol) due to the presence of 2% H_2O vapor (Fig. 9). Here, water also competes with CH_4 for reaction sites. Given the fact that both CH_4 combustion and NO reduction probably occur on the Co^{2+} sites, it is understandable that water decreases the reaction rates for both NO reduction and CH_4 combustion but not the selectivity (25).

A set of rates and turnover frequencies were measured over a series of Co–FER(8) catalysts with different levels of cobalt (Co/Al = 0.21, 0.27, 0.39, and 0.46). Because a high-temperature dehydration should drive metal ions to the exchangeable sites of a zeolite, these samples were calcined at 650°C for 4 h prior to kinetic runs, and these kinetic runs were made with very high space velocities (GHSV = 100,000–200,000) to minimize mass diffusion control and to lower NO and CH_4 conversions. [Here, the conversions were maintained below 30%.] Figure 10 shows the dependence of NO reduction rate as a function of Co/Al ratio and reaction temperature. It is obvious that H^+ form ferrierite, H–FER(8), has a much lower activity compared to Co–FER(8) catalysts, and a similar observation was reported on other H zeolites, e.g., H–ZSM-5 (2). For Co–FER(8) catalysts, the NO reduction rate is proportional to the cobalt loading in ferrierite at any given temperature, and the rate increases monotonically with temperature. Note that, unlike the rates measured at a lower space velocity (16), the rates did not bend over at 550°C with increasing temperature, suggesting that this feature is dictated by the nature of the catalyst and operating conditions at $T \leq 550$°C.

Table 3 illustrates the TOF of the NO reduction as a function of cobalt loading and temperature. Interestingly, the TOF also increases with cobalt loading at any given temperature. For example, the TOF for Co–FER(8)-92 is about 3 times of that for Co–FER(8)-42, and on all catalysts TOF increases with temperature. This demonstrates that not every Co^{2+} in ferrierite is equally active for the NO reduction with CH_4. The activity of each H^+ is negligible compared to Co^{2+} (Table 3).

Figure 11 shows the CH_4 combustion rate on the same

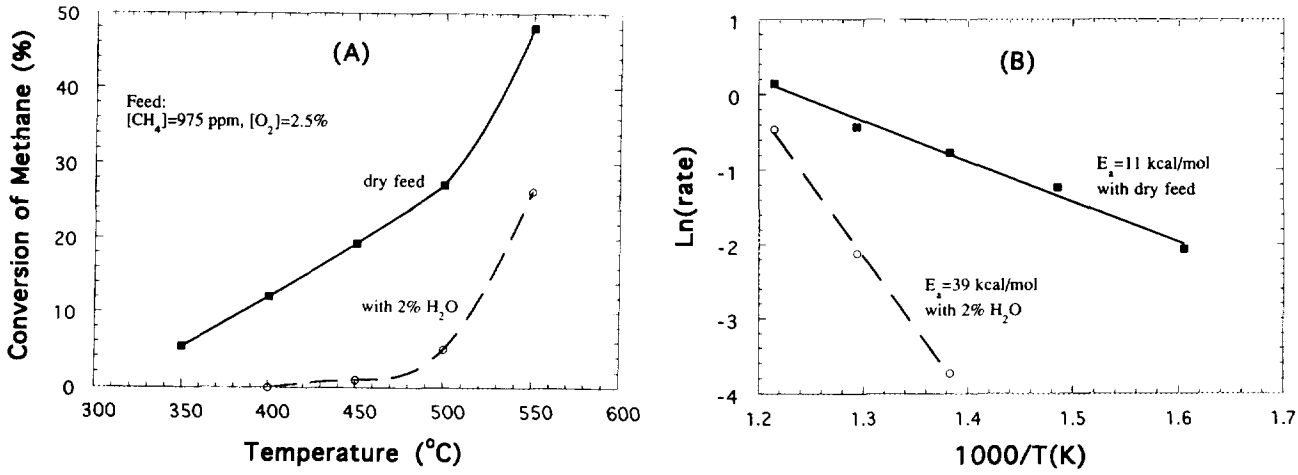

FIG. 9. Conversion–temperature plots (A) and Arrhenius plots (B) for combustion of CH_4 over Co–FER(6)-74 with a dry and wet feed.

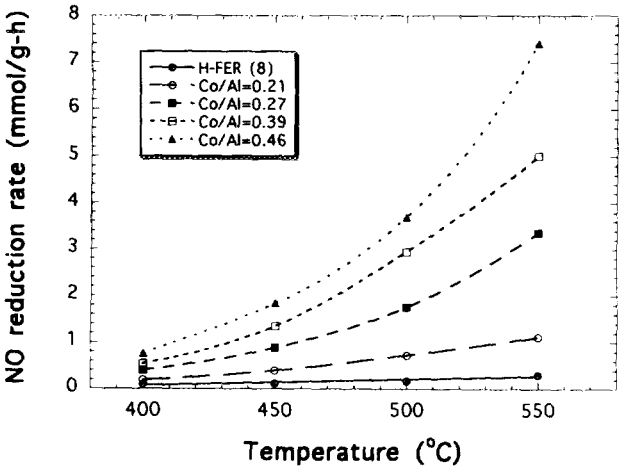

FIG. 10. NO reduction rate vs temperature as a function of Co/Al ratio in ferrierite on Co–FER(8). The NO conversions for these runs were controlled below 30%.

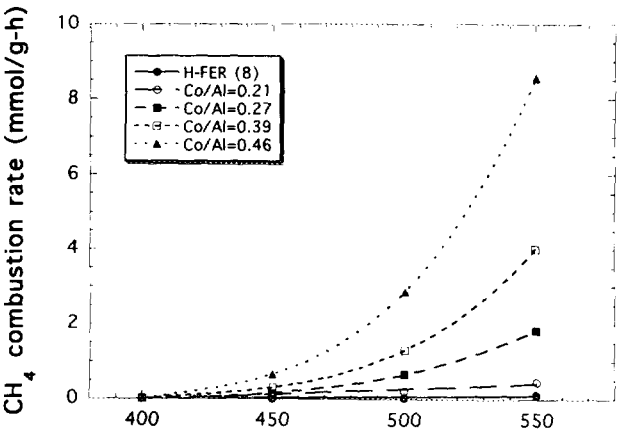

FIG. 11. CH_4 combustion rate vs temperature as a function of Co/Al ratio in ferrierite on Co-FER(8). The CH_4 conversions for these runs were controlled below 30%.

set of Co–FER(8) catalysts as a function of temperature. [Methane combustion rate was calculated as the difference between the total consumption rate and one half of the NO reduction rate (the rate of CH_4 consumption to reduce NO).] Methane combustion rate is negligible at 400°C on all catalysts, suggesting that all the CH_4 consumed at this temperature was used for reduction of NO. At $T \geq 450$°C, the CH_4 combustion rate increases dramatically with temperature and with cobalt loading. As shown in Table 4, the TOF for the CH_4 combustion also increases with cobalt loading; at 550°C, the TOF is one order of magnitude higher for Co–FER(8)-92 than for Co–FER(8)-42. Based on these measurements, the ratios of NO reduction rate to CH_4 combustion rate (r_1/r_2) are listed in Table 5 as a function of temperature. Methane is better utilized for NO reduction at a lower temperature or with a lower cobalt loading, but a low temperature or lower cobalt loading also results in a lower NO reduction rate.

TABLE 3

Turnover Frequency[a] of NO (1/sec × 1000) over Co–FER(8)

Co/Al	[Co] (mmol/g)	400°C	450°C	500°C	550°C
H–FER(8)	0	0.018	0.02	0.031	0.054
0.21	0.38	0.14	0.29	0.53	0.81
0.27	0.46	0.24	0.54	1.06	2.03
0.39	0.67	0.22	0.56	1.22	2.07
0.46	0.78	0.27	0.65	1.4	2.6

[a] Turnover frequency (TOF) is defined as the number of NO molecules converted to N_2 per second per Co^{2+} ion (per H^+ for H–FER(8)). The TOFs are calculated based on the data shown in Fig. 10.

DISCUSSION

The effect of O_2 on NO reduction rate shown in Fig. 1 clearly demonstrates that O_2 is essential for the reduction of NO with CH_4. Beyond the NO/CH_4 reaction, the enhancement of NO conversion by O_2 was noted with other hydrocarbons, e.g., C_3H_6, C_3H_8, and C_2H_4. Hamada and co-workers (18–20) first reported the promoting effect of O_2 for NO_x reduction with C_3H_8 using alumina and H–ZSM-5. Their comparative studies using NO and NO_2 with various levels of O_2 suggested that the presence of O_2 in the feed promoted the formation of NO_2, which is a better oxidant. The NO_2/CH_4 reaction rate is much higher than the rate for NO/CH_4 reaction in the absence of O_2. In the presence of excess O_2 the difference in reaction rate is reduced, and at higher temperatures, e.g., >500°C (in the presence of excess O_2), the rates for these two reactions are comparable.

Our experiment using NO_2 (Fig. 2) also suggests that catalyst-bound NO_2 species may be a reactive intermediate for the NO/CH_4/O_2 system, and the purpose of O_2 is

TABLE 4

Turnover Frequency[a] of CH_4 for CH_4 Combustion (1/sec × 1000) over Co–FER (8)

Co/Al	[Co] (mmol/g)	400°C	450°C	500°C	550°C
H–FER(8)	0	0.0	0.0009	0.0045	0.02
0.21	0.38	0.0	0.048	0.15	0.33
0.27	0.46	0.0	0.09	0.40	1.11
0.39	0.67	0.0	0.12	0.54	1.66
0.46	0.78	0.03	0.23	1.01	3.03

[a] Calculated based on the data shown in Fig. 11.

TABLE 5

Ratio of NO Reduction rate to CH_4 Combustion Rate (r_1/r_2)[a] as a Function of Temperature and Co/Al Ratio in Co–FER(8)

Co/Al	450°C	500°C	550°C
0.21	6.0	3.4	2.4
0.27	5.9	2.7	1.8
0.39	4.5	2.3	1.2
0.46	2.8	1.4	0.9

[a] Calculated based on the data shown in Tables 3 and 4.

to generate NO_2 by reacting NO with O_2 (Eq. [5]). This oxidation reaction can occur catalytically or homogeneously in gas phase (24). Using N_2O, instead of O_2, as a gaseous promoter for the NO reduction provides more efficient oxygen atoms on catalyst via the decomposition of N_2O, and thus NO can be more effectively oxidized to NO_2.

The formation of NO_2 via NO oxidation is a thermodynamically controlled reaction and is favored at lower temperatures (<500°C). Thus, the bending over of NO_2 conversion (Fig. 3) with increasing temperature at $T > 500$°C may be explained by a lower level of NO_2 species due to thermodynamic limitations. In fact, O_2 was observed during NO_2/CH_4 reaction as a result of the decomposition of NO_2 to O_2 and NO, and some O_2 molecules further reacted with CH_4, resulting in an overconsumption of CH_4 based on Eq. [4] (see Fig. 2). This is an important factor for the conversion bending over at high temperatures with $NO/O_2/CH_4$ system. This thermodynamic explanation of the bending over phenomenon was recently described by Hall and co-workers (15), suggesting the importance of surface NO_2 species. Conceivably, the NO reduction rate or conversion at $T > 500$°C is a balance of several factors. The intrinsic reaction rate increases with temperature but the surface population of NO_2 species decreases with temperature. In addition, high temperatures result in a higher combustion rate of CH_4, thus lowering the concentration of CH_4 available for Eq. [1]. These factors are dependent on temperature, feed composition, space velocity, and the type of catalyst. Under the same reaction conditions (GHSV = 30,000, 1610 ppm NO, 1000 ppm CH_4, 2.5% O_2), we obtained optimum reaction temperatures of ~450, 500, and 600°C for Co–ZSM-5, Co–ferrierite, and Mn–ferrierite, respectively (16). However, with Co–FER(8), the bending over was not observed up to 550°C using a very high space velocity (200,000 h^{-1}) when CH_4 conversion was minimized (Table 3). The thermodynamic argument, however, cannot explain the bending over which occurred at lower temperatures. At lower temperatures (<500°C), the NO_2 formation is favored thermodynamically, and the bending over of NO conversion is mainly a function of catalyst and operating conditions. We found that at lower space velocities or with a less selective catalyst (more active for CH_4 combustion) the optimum reaction temperature tends to be lower (1). The depletion of CH_4 always dominates the bending over temperature of the NO conversion–temperature curve. This analysis is consistent with the observation by Sato *et al.* for $NO/C_2H_4/O_2$ reaction (7, 8). The order of the optimum reaction temperature for the cation-exchanged ZSM-5 zeolite was Fe(200°C) < Cu(250°C) < Co(350°C) < H(400°C) < Ag(450–650°C) < Zn(600°C).

To test whether external diffusion is important in affecting catalytic activity and the shape of the conversion–temperature curve, we checked the effect of pellet size (60/80 mesh vs 12/20 mesh) at a GHSV of 30,000 and obtained identical conversions for the two ranges of pellet size. Therefore, external diffusion control is negligible. This is evident because the pellets were formed by lightly pressing the zeolite powder without using any binder. In terms of external diffusion, the pellets are just as effective as the powder itself. The diffusion within the zeolite pores, however, should be more important, which is related to the gas molecules involved, pore dimension, and crystallite size (not pellet size) of the zeolite.

Our TPD experiments illustrate that the adsorbed NO_x species was being reduced with flowing O_2/CH_4 mixture, and the onset temperature is ~320°C (for N_2 or CO_2 formation in Fig. 3c). It follows that in order to effect the NO_x reduction, a sufficient amount of NO_x species needs to be maintained on the catalyst at the temperatures where CH_4 can be activated. These TPD experiments also illustrate that the presence of O_2 alters significantly the NO desorption profile; a small amount of NO_x species desorbs at much higher temperatures (~400°C) in an O_2/He stream than in a He stream (Figs. 3a and 3b). The high-temperature desorption species may be catalytically significant.

The TPD experiments and the steady-state CH_4 combustion data illustrate that the combustion of CH_4 is insignificant at low temperatures, i.e., $T \leq 400$°C. At lower temperatures, formation of surface NO_2 species is more favorable thermodynamically. Consequently, the surface reaction involving CH_4 activation must be crucial and may be a rate-determining step for the overall NO reduction catalysis. The NO reduction rate should increase with temperature to a point where either the competing reaction (CH_4 combustion) depletes CH_4 or the number of NO_2 species becomes very small. Thus, the overall NO reduction rate at higher temperatures must be limited by formation of surface NO_2 species not activation of CH_4. CH_4 combustion is a parallel reaction to the NO_x reduction, and it takes away CH_4 needed for the NO reduction

at higher temperatures. However, the combustion of CH_4 by O_2 may not alter the NO reduction mechanism.

Previously, we reported (25) that the reduction rate of NO over Co–ZSM-5 can be expressed by a Langmuir–Hinshelwood equation

$$\text{Reaction rate } (r) = \frac{k[NO][CH_4]}{1 + K_1[NO] + K_2[H_2O]}, \quad [6]$$

where k is the apparent rate constant, K_1 is the NO adsorption equilibrium constant, and K_2 is the H_2O adsorption equilibrium constant. [NO] and [H_2O] are concentrations of NO and H_2O, respectively. This equation was derived with an excess of O_2, where the rate is independent of O_2 concentration. This equation clearly reveals the importance of NO coverage on the Co–ZSM-5 catalyst and the competitive nature of H_2O adsorption on the catalyst sites.

The data presented in Table 2 over a Co–ferrierite catalyst are also consistent with the Langmuir–Hinshelwood form rate expression (Eq. [6]) based on Co–ZSM-5. For CH_4 partial pressure dependence and under dry conditions, a denominator term, $K_2[H_2O]$, increases with the amount of CH_4 converted and consequently with [CH_4]. Therefore, the empirical rate order in CH_4 is less than 1. With the addition of 2% H_2O, the $K_2[H_2O]$ term becomes dominant and is relatively less variant with [CH_4]. Thus the apparent order in [CH_4] increases. The lower the temperature, the higher the K_2, the adsorption equilibrium constant for H_2O. We observed that at 450°C the empirical order in CH_4 is close to unity. For NO partial pressure dependence, the denominator variable is $K_1[NO]$. The difference between $K_1[NO]$ and $K_2[H_2O]$ determines the reaction order in NO. Apparently, even with 2% H_2O at 450°C, $K_2[H_2O]$ does not dominate the denominator terms; the empirical order in NO is 0.74, which is different from that on a Co–ZSM-5 catalyst. This difference may be attributed to the different strengths for NO and H_2O adsorption, i.e., different K_1's and K_2's for these two catalysts.

The effect of H_2O addition on the NO reduction is also manifested by a sharp increase of the apparent activation energy from 22 to 34 kcal/mol. (Fig. 8). This change in apparent activation energy may be understood with aid of the reaction rate expression (Eq. [6]). Increase of reaction temperature decreases K_2, the equilibrium adsorption constant for H_2O, and therefore reduces the effect of water. In addition, the desorption of H_2O molecules creates more sites for NO reduction. Therefore, increasing temperature enhances the reaction rate more dramatically under wet conditions. In an ideal case, with excess amounts of H_2O, i.e., $K_2[H_2O] \gg 1 + K_1[NO]$, Eq. [6] can be reduced to

$$r = k_H \frac{[NO][CH_4]}{[H_2O]}, \quad (7)$$

where $k_H = k/K_2$, k (in Eq. [6]) can be expressed as $k_o \exp(-E_a/RT)$, and $K_2 = k_{ad}/k_{des} = K_o' \exp[-(E_{ad} - E_{des})/RT]$, where E_{ad} is activation energy for H_2O adsorption and E_{des} is activation energy for H_2O desorption. E_{ad} is close to 0 for H_2O, and, therefore, K_2 is proportional to $\exp(E_{des}/RT)$. Hence, k_H is proportional to $\exp[-(E_a + E_{des})/RT]$. The activation energy for NO reduction in the excess of H_2O would be $E_a + E_{des}$.

Although the reaction rate equation for $CH_4 + O_2$ on the Co–ferrierite catalyst was not determined, Fig. 9a clearly demonstrates that this reaction is strongly inhibited by H_2O. At 500°C, the CH_4 conversion is only 5% with the presence of 2% H_2O (vs 27% with a dry feed). Since the CH_4 combustion activity on H–ferrierite is negligible under these reaction conditions (16), the combustion must be catalyzed on cobalt sites. The above analysis on activation energy change for NO reduction can also be used for the activation energy change (11 to 39 kcal/mol upon addition of 2% H_2O) for the CH_4 combustion. Because H_2O decreases the rates for both NO reduction and CH_4 combustion, the selectivity for the use of CH_4 for NO reduction is not affected by the water addition.

Based on the above kinetic studies with H_2O and others reported earlier (25), it is not difficult to draw a conclusion about the nature of H_2O on the NO reduction catalysis. Water, either generated by the reaction or added in the feed, merely reduced the number of Co^{2+} sites available for the NO reduction (and CH_4 combustion). As the temperature increases, the number of adsorbed H_2O molecules decreases (more sites available for NO reduction), and the effect of H_2O on the overall NO reduction rate becomes insignificant. However, the presence of H_2O does not alter the NO reduction mechanism, e.g., rate-determining step.

We reported earlier that all Co-containing zeolites display a volcano-shaped curve for conversion vs temperature (1, 2), and at any given temperature, there is an optimum Co loading beyond which the conversion drops (2, 16). It is important to realize that these phenomena are associated with experimental conditions, i.e., under integral reactor conditions. These phenomena can be avoided or altered by making the kinetic runs under low conversion conditions (high space velocities). Thus the rates and trends observed in Tables 3–5 are close to the intrinsic activities of Co^{2+} cations in ferrierite.

One of the most interesting and intriguing observations is that the TOF for the catalyst with Co^{2+} exchange level of 42% (Co/Al = 0.21) is significantly lower than that with 54% Co^{2+} exchange level (Co/Al = 0.27) (see Table 3). This may be rationalized by analyzing the topology of

ferrierite. Ferrierite has a two-dimensional channel system with a 10-ring channel (4.3 × 5.5 Å) on the [001] plane and an 8-ring channel (3.5 × 4.8 Å) on the [010] plane (30). The number of cation sites in 10-rings and in 8-rings should be comparable. We suspect that cations were preferentially located on the sites in 8-rings after a high-temperature (650°C) calcination. Those sites are thermodynamically more stable with higher coordinations compared to 10-rings. After sites in 8-rings are filled, the cation occupies the 10-ring sites. By comparing the activity and selectivity of Co–ZSM-5 and Co–ferrierite, we suspect that at low temperatures (400–450°C) sites in 8-rings are less active for NO reduction but more selective for the use of CH_4 relative to the sites in 10-rings where CH_4 combustion is enhanced. At high temperatures, the activity of Co^{2+} in the 8-ring sites should increase, whereas the activity for Co^{2+} in the 10-ring sites may not reach the level expected due to the combustion of CH_4 which lowers $[CH_4]$ in these channels.

Zeolite ZSM-5, on the other hand, has a two-dimensional, 10-ring channel system with a ring size of 5.6 × 5.3 Å for the straight channels, [001] plane, and 5.1 × 5.5 Å for the sinusoidal channels, [100] plane (26). The cation sites are probably equivalent in both channels, and TOF should be independent of the Co^{2+} exchange level. This is indeed what we observed previously (2); the turnover frequencies for NO reduction were constant for Co^{2+} exchange levels from 44 to 66% in a temperature range of 400–500°C. Ferrierite also has a higher cation exchange capacity than ZSM-5 because of its higher Al content (Si/Al = 6 or 8 for ferrierite, Si/Al = 14 for ZSM-5). At $T \leq$ 450°C, these two catalysts have comparable overall activities for the NO reduction (16). However, at high temperatures Co–ferrierite is superior to Co–ZSM-5. We suggest that the high selectivity (and consequently high activity) for Co–ferrierite at higher temperatures ($T >$ 450°C) is the result of an 8-ring structure in ferrierite. At high temperatures, the more open channels tend to be more active for CH_4 combustion, which reduces the effective CH_4 concentration in reactor. In this regard, the diffusivity in different channels may play an important role for the NO reduction. The even lower selectivity observed on Co–mordenite compared to Co–ZSM-5 can be attributed to its 12-ring channel system.

CONCLUSIONS

The formation of a catalyst-bound NO_2 species is considered a necessary step for the NO reduction with CH_4 on a Co–ferrierite catalyst. This NO_2 species can be formed by reacting NO with O_2 catalytically (or homogeneously) or by reacting with O atoms resulted from N_2O decomposition on the same catalyst. The bending over of NO_x conversion at $T > 500$°C is mainly caused by the disappearance of this NO_2 species due to its thermodynamic limitation, while the bending over at lower temperatures may result from the depletion of CH_4 in feed. Like Co–ZSM-5, the kinetics on Co–ferrierite catalysts can be described by a Langmuir–Hinshelwood equation. The presence of H_2O vapor decreases both NO reduction and CH_4 combustion rate by physically occupying the active sites, and this effect diminishes at high temperatures. The turnover frequency of Co–ferrierite is strongly dependent on the exchange level and therefore on the siting and coordination of Co^{2+} in zeolite. Optimum Co^{2+} level can be determined by balancing the NO_x conversion and the selectivity for CH_4 utilization.

ACKNOWLEDGMENTS

Thanks are due to Paula Battavio for the activity measurements and to Tom Farris for catalyst preparations. We thank Air Products and Chemicals, Inc. for permission to publish this work.

REFERENCES

1. Li, Y., and Armor, J. N., *Appl. Catal. B* **1,** L31 (1992).
2. Li, Y., and Armor, J. N., *Appl. Catal. B* **2,** 239 (1993).
3. Adlhart, O. J., Hindin, S. G., and Kenson, R. E., *Chem Eng. Prog.* **76,** 73 (1971).
4. d'Itri, J. L., and Sachtler, W. M. H., *Catal. Lett.* **15,** 289 (1992).
5. Iwamoto, M., *in* "Future Opportunities in Catalytic and Separation Technologies" (M. Misono, Y. Moro-oka, and S. Kimura Eds.), p. 121. Elsevier, Amsterdam, 1990.
6. Li, Y., and Hall, W. K., *J. Catal.* **129,** 202 (1991).
7. Sato, S., Yu-u, Y., Yahiro, H., Mizuno, N., and Iwamoto, M., *Appl. Catal.* **70,** L1 (1991).
8. Sato, S., Hirabay, H., Yahiro, H., Mizuno, N., and Iwamoto, M., *Catal. Lett.* **12,** 193 (1992).
9. Bennett, C. J., Bennett, P. S., Golunski, S. E., Hayes, J. W., and Walker, A. P., *Appl. Catal. A* **86,** L1 (1992).
10. Ansell, A. P., Diwell, A. F., Colunski, S. E., Hayes, J. W., Rajaram, R. R., Truex, T. J., and Walker, A. P., *Appl. Catal. B* **2,** 81 (1993).
11. Burch, R., and Millington, P. J., *Appl. Catal. B* **2,** 101 (1993).
12. Iwamoto, M., Mizuno, N., and Yahiro, H, *in* "Proceedings, 10th International Congress on Catalysis, Budapest, 1992" (L. Guczi, F. Solymosi, and P. Tétényi, Eds), p. 1285. Akadémiai Kiadó, Budapest, 1993.
13. Held, W., Konig, A., Richter, T., and Ruppe, L., SAE Paper No. 900496, 1990.
14. Bartholomew, C. H., Gopalakrishnan, R., Stafford, P. R., Davison, J. E., and Hecker, W. C., AIChE 1992 Annual Meeting, Nov. 1–6, 1992, Miami Beach, FL. Paper No. 240a.
15. Petunchi, J., Sill, G., and Hall, W. K., *Appl. Catal. B* **2,** 303 (1993).
16. Li, Y., and Armor, J. N., *Appl. Catal. B* **3,** L1 (1994).
17. Li, Y., and Armor, J. N., *J. Catal.* **150,** 388 (1994).
18. Hamada, H., Kintaichi, Y., Sasaki, M., Ito, T., and Tabata, M., *Appl. Catal.* **64,** L1 (1990).

19. Kintaichi, Y., Hamada, H., Tabata, M., Sasaki, M., and Ito, T., *Catal. Lett.* **6,** 39 (1990).
20. Hamada, H., Kintaichi, Y., Sasaki, M., Ito, T., and Tabata, M., *Appl. Catal.* **70,** L15 (1991).
21. Misono, M., and Kondo, K., *Chem. Lett.*, 1001 (1991).
22. Li, Y., and Armor, J. N., U.S. Patent No. 5,171,553 (1992).
23. Li, Y., and Armor, J. N., *Appl. Catal. B.* **3,** 55 (1994).
24. Li, Y., and Hall, W. K., *J. Phys. Chem.* **94,** 6145 (1990).
25. Li, Y., Battavio, P. J., and Armor, J. N., *J. Catal.* **142,** 561 (1993).
26. Meier, W. M., and Olson, D. H., *in* "Atlas of Zeolite Structure Types," 3rd ed. Butterworth-Heinemann, London, 1992.